Article

A rationally designed microbial consortium modulates neurodegeneration in a *Drosophila melanogaster* model of Parkinson's disease

Check for updates

Aline Ovalle[1], Estefanía López[2,3], Jimena Sierralta[2,3] ✉, Nuria Paricio[4] ✉ & Daniel Garrido[1] ✉

The gut-brain axis enables communication between the central nervous system and the gut, with certain microbial metabolites influencing neurodegeneration. Using genome-scale metabolic modeling, we designed and tested a synthetic microbial consortium with predicted capacity to produce GABA and other neurometabolites in a *Drosophila melanogaster* model of neurodegeneration of Parkinson's Disease (PD). The consortium (*Levilactobacillus brevis*, *Lacticaseibacillus paracasei*, *Bacteroides thetaiotaomicron*) produced GABA in bioreactors. Female PD flies receiving the consortium exhibited protection from locomotor impairment at 10 and 25 days upon consortium administration. Head metabolomics revealed partial restoration of PD-associated alterations in energy balance, amino acid and neurotransmitter metabolism, and disease-related biomarkers. Early administration increased microbiome diversity and *Lactobacillus* abundance. These findings suggest that rationally designed microbial consortia targeting neurometabolite production can modulate brain physiology and confer neuroprotection, supporting their potential for microbiome-based interventions in neurodegenerative disease.

The human gut microbiome comprises a set of genomes of commensal and symbiotic microorganisms found in the gastrointestinal tract that coexist with the host, influence gut homeostasis, and play an essential role in health[1]. Changes in their composition are associated with the development of various conditions such as intestinal, metabolic, and immune diseases[2,3]. In recent years, the impact of the gut microbiome on psychiatric disorders and neurodegeneration has been evidenced[4]. A bidirectional communication between the brain and the gut, the gut-brain axis, has been described[5]. Here, the central nervous system (CNS) influences the gastrointestinal tract's motor, sensory, and secretory functions, while signals from the gut microbiome can impact nervous system functions[5]. This communication is possible through pathways such as the vagus nerve, the hypothalamic-pituitary-adrenal axis, and microbial metabolites such as short-chain fatty acids

(SCFAs) and neurotransmitters[6–9]. Butyrate, one of the most critical SCFAs for host health, can improve intestinal barrier function, stimulate the immune system, and reduce inflammation[10]. It also displays a neuroprotective effect on the nervous system[11–13]. Additionally, some gut microbes synthesize neurotransmitters de novo[14], such as dopamine, serotonin, norepinephrine, and γ-aminobutyric acid (GABA), the primary inhibitory neurotransmitter of the CNS[15,16]. This property is distributed among gut microbes, especially in *Bacteroides*, *Lactobacillus*, and *Bifidobacterium*[17], which use this compound as a cross-feeding molecule or growth factor, and to regulate physiological processes such as acid stress[18,19].

Reductions in brain GABA have been associated with anxiety, depression[20–24], and neurodegeneration[25–27]. Remarkably, GABA-producing bacteria species *Lactobacillus* and *Bifidobacterium* delivered in the gut of

[1]Department of Chemical and Bioprocess Engineering, School of Engineering, Pontificia Universidad Católica de Chile, Av. Vicuña Mackenna, 4860 Santiago, Chile. [2]Department of Neuroscience, Faculty of Medicine, Universidad de Chile, Independencia 1027, Santiago, 8380453, Chile. [3]Biomedical Neuroscience Institute, Faculty of Medicine, Universidad de Chile, Independencia 1027, Santiago, 8380453, Chile. [4]Department of Genetics, Biological Sciences Faculty and University Institute for Biotechnology and Biomedicine (BIOTECMED) Research, Universidad de Valencia, 46100 Burjassot, Spain. ✉e-mail: jsierral@uchile.cl; nuria.paricio@uv.es; dgarridoc@ing.puc.cl

aging rats modulate the brain metabolic profile in the frontal cortex and hippocampus, inducing beneficial effects on memory[28]. In rats receiving these bacteria, GABA concentrations increased in the frontal cortex, which could modulate glutamate neurotransmission and synaptic plasticity[28]. Another study showed that the abundance of GABA-producing bacteria, such as *Bifidobacterium* and *Lactobacillus* species, decreased in the gut microbiome of fibromyalgia patients, along with glutamate accumulation and GABA depletion[26]. Genes participating in GABA synthesis (*gadC* and *gadB*) were also downregulated[26]. Considering that lactic acid bacteria produce high concentrations of lactate and acetate, these molecules could also contribute to these neuroprotective effects, but their impact remains mostly uncharacterized.

The effect of different dietary bacteria on the nervous system was recently evaluated in *Caenorhabditis elegans*. The results indicated that *Escherichia coli* HT115 exerted a neuroprotective effect through GABA production since mutants lacking the *gad* were not neuroprotective[27]. These results highlight the potential role of microbial neurometabolites in the nervous system and position them as potential candidates to evaluate their impact on neurodegenerative disorders by gut microbiome modulation.

Clinical and preclinical evidence suggest that microbial composition changes in the gut may increase the risk of neurodegenerative diseases[4]. The fecal metabolome from patients with Parkinson's disease (PD) shows that alterations in their gut microbiome correlate with changes in the metabolites produced by bacterial species. Specifically, changes in the secretion of specific metabolites, including GABA, were observed[25]. A correlation between Parkinson's disease and gut microbiome alterations in patients has been shown[29]. A large-scale cohort study including 72 PD patients and the same number of healthy controls suggested that *Prevotellaceae* abundance was decreased in PD patients[30]. Also, the abundance of butyrate-producing bacteria, such as *Roseburia* and *Faecalibacterium* spp., was significantly reduced in PD patients compared to healthy controls[31]. Interestingly, evidence linked PD with α-synuclein accumulation in the gastrointestinal tract[4]. Therefore, interventions targeting the gut microbiota, such as fecal microbiota transplantation (FMT) and probiotic and prebiotic administration, have been evaluated in PD patients[32,33].

Despite these findings, the role of microbial metabolites such as GABA or SCFAs in neurodegeneration remains unclear, especially in PD, which targets primarily dopaminergic neurons. While microbial GABA production has been demonstrated in vitro, its functional role in vivo, particularly in neuroprotection, remains speculative. We hypothesize that a microbial consortium capable of producing neuroactive metabolites such as GABA and related metabolites such as lactate could mitigate some markers of neurodegeneration. In this study, we aimed to evaluate the impact of a putative neuroactive microbial consortium on a genetic PD model in *Drosophila melanogaster*, a well-established system for studying neurodegenerative processes[34–37]. *D. melanogaster* offers significant advantages, including a short lifecycle, powerful genetic tools, cost-effectiveness, and conserved disease pathways replicating key hallmarks of human neurodegenerative conditions. We used metabolic modeling to design a microbial consortium with predicted capacity to produce GABA and other neurometabolites and evaluated its effects on *D. melanogaster* with α-synuclein overexpression, which mirrors PD-like phenotypes.

Results

SteadyCom simulations revealed GABA and butyrate-producing consortia

This study aimed to understand the impact of neurometabolite-producing microbial consortia in a neurodegeneration model in *D. melanogaster*. We first focused on GABA and butyrate for their role in neuroprotection. We first obtained semi-automatic metabolic reconstructions of nine candidate gut microbes chosen for their GABA production, interactions with GABA producers from the genera *Bifidobacterium*, *Lactobacillus* or *Bacteroides*, or Butyrate-Producing Bacteria (Supplementary Table 1[38]). All reconstructions predicted biomass production on glucose, and *B. thetaiotaomicron* and *B. adolescentis* produced biomass using inulin as the carbon source (Table 1),

with higher growth rates generally observed in glucose. A few models showed positive in silico GABA fluxes (Table 1): *Bifidobacterium adolescentis*, *Bacteroides thetaiotaomicron* and *Lactiplantibacillus plantarum*. While *Levilactobacillus brevis* G2 did not exhibit GABA production in monoculture simulations, its model reconstruction contained both the synthesis and export reaction for GABA (Table 1), consistent with previous reports[17].

We then used these models to simulate multispecies consortia, evaluating community growth, metabolite production, and metabolic cross-feeding. We assembled and tested combinations involving primary and secondary fermenters, as well as predicted GABA- or butyrate-producing strains. These simulations yielded 23 consortia with predicted GABA production using glucose or inulin (Table 1). Notably, growth rates were inversely correlated with GABA fluxes (Table 1). Increasing the number of bacteria in the consortia did not necessarily increase growth rates or GABA production. Some consortia exhibited high GABA and butyrate fluxes. For instance, a consortium composed of *B. adolescentis*, *Coprococcus eutactus*, *B. thetaiotaomicron and L. brevis* produced high GABA (Consortium 9; 1.48 mmol gDW^{-1}h^{-1}) and butyrate fluxes (4.39 mmol gDW^{-1}h^{-1}). In general, *L. brevis* and *L. plantarum* contributed the most to GABA production in silico.

Flux Variability Analysis (FVA) was later used to explore suboptimal metabolic states and confirm community metabolic flexibility. In Consortium 9, although three members harbored GABA synthesis capacity (Supplementary Fig. 1A), only two actively produced the neurometabolite at the optimal growth rate (Supplementary Fig. 1B). As community growth increased, GABA fluxes decreased, suggesting a trade-off between community biomass optimization and neurometabolite output. FVA analysis of Consortium 9 revealed that cross-feeding of acetate, lactate, and glutamate supported GABA and butyrate production (Fig. 1A), resulting in a complex interaction network (Fig. 1C).

In some consortia, GABA was predicted to be produced before reaching the maximum community growth rate (Supplementary Fig. 1C). For example, a consortium formed by *L. brevis*, *B. thetaiotaomicron*, and *Lacticaseibacillus paracasei* (C8c) showed equal relative abundances of these species at low growth rates (Supplementary Fig. 1C). This consortium displayed no GABA flux at optimum growth rates, but GABA flux was rather significant at suboptimal rates (Supplementary Fig. 1D). As above, cross-feeding of acetate, lactate, and glutamate appears necessary for GABA production in silico in some microbial consortia (Fig. 1B).

GABA screening showed GABA production in monoculture and co-culture

Based on simulation results, we screened 15 monocultures, 11 co-cultures, eight tri-cultures, and two tetra-cultures for GABA production. GABA was detected in eight supernatants, including *L. brevis* G2 and *B. thetaiotaomicron* VPI 5482 (Fig. 2A). Notably, the co-culture of *L. brevis* G2 and *L. paracasei* M38 produced GABA independent of monosodium glutamate supplementation (Fig. 2B). However, adding monosodium glutamate intensified the GABA band (Fig. 2B), suggesting that substrate availability can potentiate production in vitro.
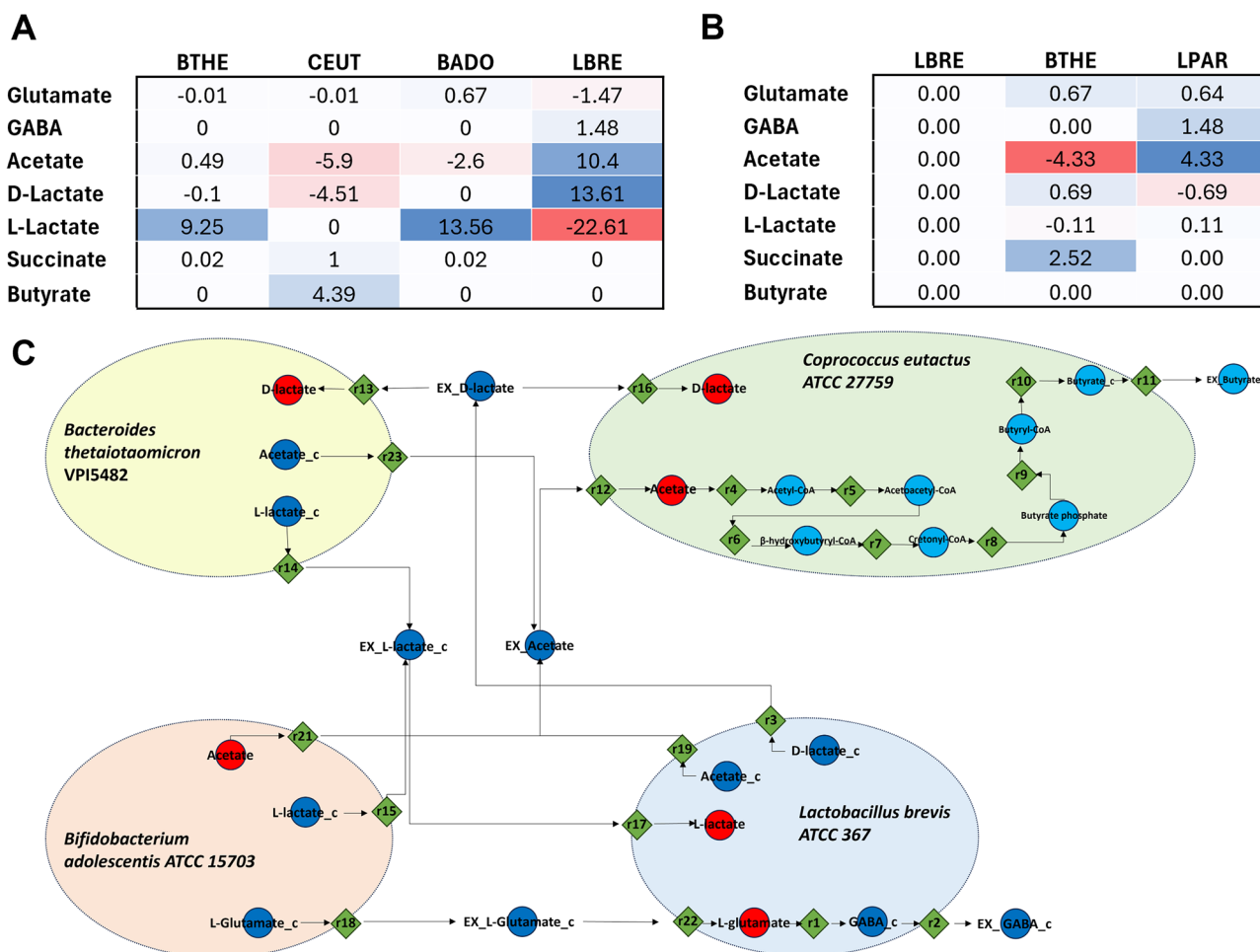
Consortia batch bioreactor growth and substrate consumption

Six microbial consortia producing GABA in silico were selected for batch fermentations using inulin as a carbon source: G2M38, BvulgM38, G2BtM38, G2BovaM38, D3BtM38 and BtLsG2M38 (G2: *L. brevis* G2; M38: *L. paracasei* M38; Bvulg: *Phocaeicola vulgatus* S1; Bt: *B. thetaiotaomicron* VPI 5482; Bova: *Bacteroides ovatus* BEI 3_8_47FAA; D3: *B. adolescentis* D3; Lsym: *Lachnoclostridium symbiosum* WAL14673; Supplementary Table 1). Biological replicates showed similar behavior regarding growth kinetics (Supplementary Fig. 2). Consortia with four bacteria reached the exponential phase faster (Supplementary Fig. 2). Inulin was partially consumed in most consortia by 12 h, being nearly exhausted by 26 h (Supplementary Fig. 3). The consortium BtLsG2M38 showed a faster consumption at 12 h, correlating with its shorter lag phase (Supplementary Fig. 3). These

Table 1 | Results of growth simulations of single (S) and co-culture (C) of candidate GABA-producers using metabolic reconstructions

Consortium	Composition	Medium	Growth rate (h^{-1})	GABA (mmol $gDW^{-1}h^{-1}$)	Butyrate (mmol $gDW^{-1}h^{-1}$)
S1	LSYM	INU	0.06	0	0
S2	LSYM	GLC	0.30	0	0
S3	CEUT	INU	0.00	0	0
S4	CEUT	GLC	0.21	0	3.32
S5	PDOR	INU	0.20	0	0
S6	PDOR	GLC	0.56	0	0
S7	BTHE	INU	0.82	0.82	0
S8	BTHE	GLC	0.82	0.82	0
S9	LBRE	INU	0.16	0	0
S10	LBRE	GLC	0.78	0	0
S11	LPLA	INU	0.00	0	0
S12	LPLA	GLC	0.34	0	0
S13	BADO	INU	0.25	1.21	0
S14	BADO	GLC	0.55	0.35	0
S15	LPAR	INU	0.11	0	0
S16	LPAR	GLC	0.34	0	0
S17	PVUL	INU	0.28	0	0
S18	PVUL	GLC	0.79	0	0
C1a	BADO-BTHE	INU	0.33	0.66	0
C2a	BADO-BTHE-PVUL	INU	0.37	1.34	0
C1b	LPLA-CEUT	GLC	0.28	0.73	1.54
C2b	LBRE-CEUT	GLC	0.25	1.49	3.06
C3b	LPLA-CEUT-BADO	GLC	0.30	1.37	1.47
C4b	LBRE-CEUT-BADO	GLC	0.29	1.48	2.93
C5b	LPLA-LBRE-CEUT	GLC	0.30	1.37	0.74
C6b	LPLA-BTHE-BADO-CEUT	GLC	0.31	1.36	2.63
C7b	LPLA-BADO-CEUT	GLC	0.30	1.35	1.96
C8b	LPLA-LBR-CEUT-BADO	GLC	0.29	1.45	1.96
C9b	LBRE-BTH-CEUT-BADO	GLC	0.28	1.48	4.39
C10b	LBR-BDOR-CEUT-BADO	GLC	0.29	1.63	2.47
C11b	BADO-CEUT	INU	1.23	0.87	0.05
C12b	LPLA-CEUT-BADO-LBRE-BTH	GLC	0.30	1.35	1.98
C13b	LPLA-CEUT-BTH-BADO-LBRE	GLC	0.29	1.43	2.29
C14b	LPLA-CEUT	GLC	0.30	1.36	2.63
C1c	LBRE-LPAR	GLC	0.31	0.66	0
C2c	LPLA-LPAR	INU	0.43	1.22	0
C3c	BADO-LPAR	INU	0.55	1.21	0
C4c	BTHE-LPAR	GLC	0.31	0.66	0
C5c	BADO-BTHE-LPAR	INU	1.22	0.78	0
C6c	PVUL-LPAR	GLC-INU	0	0	0
C7c	LBRE-BTHE	GLC-INU	0	0	0
C8c	LBRE-BTHE-LPAR	INU	1.14	0	0
C9c	LSYM-BADO-LPAR	INU	1.16	0	5.77
C10c	LPLA-LSYM-BADO	INU	1.22	0	1.19
C11c	PDOR-LSYM-BADO	INU	1.23	0.38	0.73
C12c	PDOR-LSYM-BADO-LPAR	INU	0	0	0
C13c	LBRE-LPAR-BTHE-LSYM	INU	0	0	0

Three rounds of simulations are shown (a, b, c). Models and abbreviations used are indicated in Supplementary Table 1, and inulin (INU) or glucose (GLC) were used in silico.

A

	BTHE	CEUT	BADO	LBRE
Glutamate	-0.01	-0.01	0.67	-1.47
GABA	0	0	0	1.48
Acetate	0.49	-5.9	-2.6	10.4
D-Lactate	-0.1	-4.51	0	13.61
L-Lactate	9.25	0	13.56	-22.61
Succinate	0.02	1	0.02	0
Butyrate	0	4.39	0	0

B

	LBRE	BTHE	LPAR
Glutamate	0.00	0.67	0.64
GABA	0.00	0.00	1.48
Acetate	0.00	-4.33	4.33
D-Lactate	0.00	0.69	-0.69
L-Lactate	0.00	-0.11	0.11
Succinate	0.00	2.52	0.00
Butyrate	0.00	0.00	0.00

C

Fig. 1 | Design of microbial consortia. A Predicted flux (mmol gDW^{-1}h^{-1}) of key metabolites and their cross-feeding at optimal growth rate for Consortium 9. BTHE: *B. thetaiotaomicron*, CEUT: *C. eutactus*, BADO: *B. adolescentis*, LBRE: *L. brevis*, LPAR: *L. paracasei*. Blue cells indicate predicted metabolite release into the extracellular medium, and red cells indicate uptake by the bacterium. B predicted flux of key metabolites and their cross-feeding at optimal growth rates for Consortium C8c. C Network representation of predicted cross-feeding across members of Consortium 9. Export metabolites are shown in blue, uptake metabolites are shown in red, and green diamonds indicate specific metabolic or exchange reactions for these metabolites. EX indicates exchange metabolites.

dynamics are likely driven by *L. paracasei* M38, which encodes inulin-degrading enzymes[38].

GABA production peaked at the end of fermentation. G2BtM38 and G2BovaM38 consortia exhibited higher GABA production in vitro (Supplementary Fig. 4). Two of the six consortia synthesized GABA (3 g/L): G2BtM38 and BtLsG2M38 (Supplementary Fig. 4D; $p = 0.0142$ and $p = 0.0120$ respectively). *L. paracasei* M38 was dominant in the three-species consortium (Supplementary Fig. 5). In contrast, the four-species consortium was dominated by *L. symbiosum* WAL 14673 and *L. paracasei* M38, which increased its abundance throughout the fermentation (Supplementary Fig. 5).

Regarding SCFA production, the consortium BtLsG2M38 produced butyrate at a concentration of 1.88 g/L (Supplementary Fig. 6). This consortium also generated the highest acetate concentration (Supplementary Fig. 6), even compared to BtG2M38. High levels of lactate, another potential neurometabolite, were observed in consortia containing *L. paracasei* M38, and succinate was characteristic of consortia containing *Bacteroides* species (Supplementary Fig. 6). Based on these results, the consortium G2BtM38, resulting in high lactate and GABA production, was selected to evaluate its impact on a neurodegeneration model in *D. melanogaster*.

Effect of the neuroactive consortium on locomotor deficits, survival, and dopaminergic degeneration in *D. melanogaster*

The effect of the selected consortium on neurodegeneration was evaluated in vivo using a genetic PD model in *D. melanogaster*. This model is based on the overexpression of α-synuclein with aggregation properties (A30P[39];). Here, flies display a PD-like phenotype, with locomotor deficits, loss of dopaminergic neurons, and premature death[40,41]. Four groups were evaluated in parallel: untreated control and PD groups (C; PD), and control and PD groups receiving the microbial consortium in the larval stage (C + ; PD +).

We tested the locomotor ability of female flies in a climbing assay on day 10 and day 25[42]. As expected, PD flies had significantly reduced climbing compared to the control group C (Fig. 3A, Fig. 3B; Two way ANOVA, Tukey's multiple comparisons test, $n = 135$ per group, $p = 0.0003$ and $p = 0.0356$ at 10 and 25 days, respectively), showing a detriment in climbing probably due to α-synuclein overexpression. In contrast, PD flies treated with the consortium (PD +) showed a significantly improved climbing index compared to untreated PD flies ($p = 0.0246$ and $p = 0.0444$ at 10 and 25 days, respectively), and were statistically indistinguishable from control groups (C and C + ; all $p > 0.1$). These results suggest that early-life exposure to the microbial consortium mitigates locomotor decline in PD flies, resulting in a neuroprotective effect.

We later evaluated the total number of dopaminergic neurons in female flies by immunostaining using anti-tyrosine hydroxylase, the enzyme required to synthesize dopamine from tyrosine (Fig. 3C). Brain images for other groups are shown in Supplementary Fig. 7. At day 25, flies expressing α-Syn had significantly fewer TH-positive dopaminergic neurons than controls (C and C + ; Fig. 3D). The PD+ group showed an intermediate

Fig. 2 | GABA screening. A Thin-layer chromatography of bacteria supernatants. The first two lanes correspond to the standards of GABA and monosodium glutamate (MSG). The following four lines are the culture media without bacteria. The remaining lines correspond to bacterial supernatant from monoculture growth. GABA is visualized as an intensely colored band at the same height as the GABA standard. All media was supplemented with monosodium glutamate (glut) to induce GABA production. Culture medium was mZMB unless indicated, and media abbreviations are indicated in methods. D3: *B. adolescentis* D3. Ba: *B. adolescentis* ATCC 15703. G2: *L. brevis* G2. L: *L. plantarum* JDM1. S1: *P. vulgatus* S1. Bt: *B. thetaiotaomicron* VPI 5482, and Bova: *B. ovatus* BEI 3_8_47FAA. **B** Thin-layer chromatography of co-cultures. BtM38: *B. thetaiotaomicron* VPI 5482 and *L. paracasei* M38. BovaM38: *B. ovatus* BEI 3_8_47FAA and *L. paracasei* M38. G2M38: *L. brevis* G2 and *L. paracasei* M38. Lanes are as in A indicating the carbon source (Glucose or Inulin).
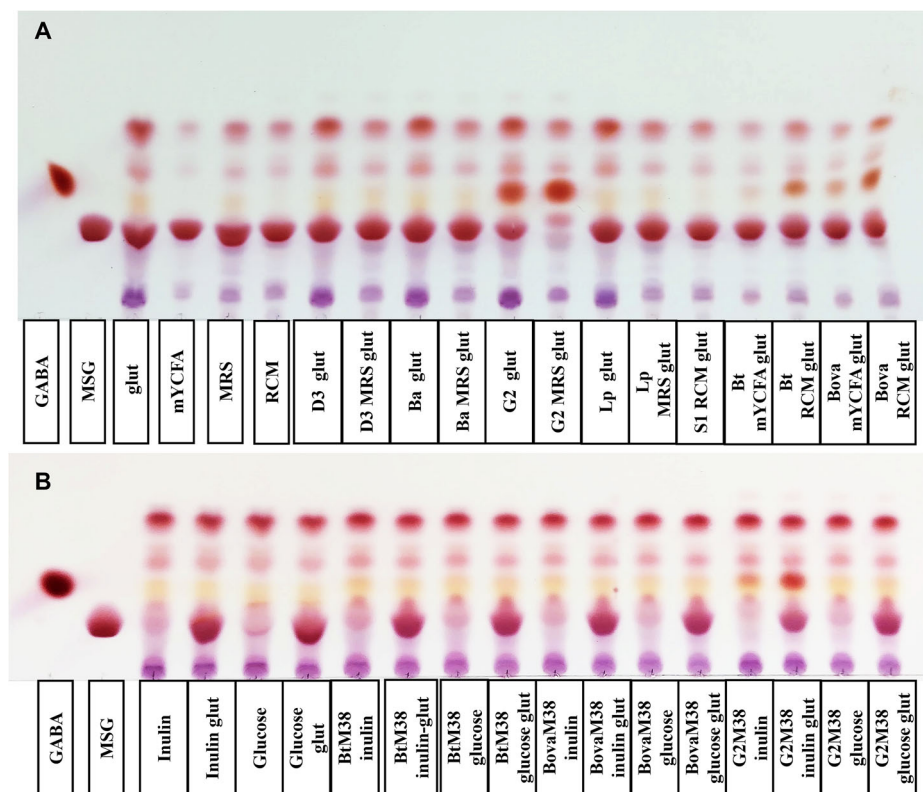
phenotype, with no significant differences compared to either controls or the untreated PD group, suggesting a partial preservation of dopaminergic neurons following consortium treatment.

Finally, survival was evaluated using male flies (Supplementary Fig. 8). No significant differences in survival were found among the four groups (Supplementary Fig. 8A, Log-rank test, n per group = 60, $x^2 = 3.784$, df = 1, $p = 0.0518$). However, when comparing control flies with and without the consortium, increased survival was associated with the consortium (Supplementary Fig. 8B, Logrank test, n per group=60, $x^2 = 4.376$, df = 1, $p = 0.0365$). Although survival results cannot be directly compared to female flies, this result shows that feeding a consortium of human commensal bacteria to *D. melanogaster* has no deleterious effect on survival of male flies.

Microbial consortia impact on the brain metabolic profiles

To investigate whether the microbial consortium influenced brain metabolism in a manner consistent with the improved locomotor performance observed in treated flies, we performed untargeted metabolomic profiling of female fly heads across all experimental groups at day 10. A three-dimensional principal component analysis (PCA) of metabolite profile distribution showed that samples were grouped by phenotype, where PD+ flies had profiles separated from the PD group (Supplementary Fig. 9). All comparisons yielded optimal models with R^2 values close to 1 and reasonable predictive values (Q^2).

NMR analysis detected a total of 33 metabolites, with 15 showing a significant difference in pairwise comparisons (One-way ANOVA with Tukey post-hoc analysis, $p < 0.05$; Fig. 4; Supplementary Table 2). The PD brain metabolome was the most distinct, while metabolomes from C+ and PD+ groups clustered more closely, suggesting a partial shift toward a shared metabolic state following consortium treatment (Supplementary Fig. 10).

Figure 4 and Supplementary Table 2 show metabolite distributions across samples and groups. GABA levels were moderately elevated in PD flies compared to controls, but its concentrations in brain were not modulated by the consortium. Lactate was significantly increased in PD+

compared to C+ , suggesting a shift in glycolytic activity (Fig. 4). In contrast, acetate levels were consistently reduced in both C+ and PD+ groups relative to their groups without consortium, suggesting the consortium is responsible for this change. Interestingly, succinate levels were significantly higher in both groups flies receiving the consortium (C+ and PD+) than untreated flies (Fig. 4), possibly reflecting improved mitochondrial function.

Certain metabolites previously associated with neurodegeneration and oxidative stress showed robust changes. N-acetylcysteine and xanthurenate were significantly elevated in both PD and PD+ flies compared to their controls, but were not modified by the consortium, suggesting persistent redox imbalance. Methionine sulfoxide and GPC, typically increased in PD, were significantly reduced in PD+ flies, indicating a partial shift toward a less oxidatively stressed state[43–45].

Amino acid-related metabolites also showed distinct profiles. Glutamine was significantly higher in PD and C+ flies compared to control, while histidine was lower in PD flies vs C. These alterations were not affected by consortium administration. Finally, metabolites related to energy metabolism and turnover were moderately affected. AMP, glycine, and glycogen were significantly reduced in C+ flies relative to controls, and glycogen was also lower in PD compared to C, suggesting alterations in energy reserves and purine metabolism linked to both disease and early-life microbial exposure. Together, these data indicate that the microbial consortium selectively modulates brain metabolism, especially in pathways related to mitochondrial activity, oxidative stress, and energy regulation. However, neurotransmitter-related metabolites such as GABA were not significantly altered by the intervention, suggesting indirect or alternative mechanisms underlying the observed neuroprotective effects.

16S rRNA profiling of the *D. melanogaster* microbiome

To assess whether the microbial consortium colonized the *D. melanogaster* gut, we performed 16S rRNA sequencing on 10 day-old female flies from all experimental groups. Taxonomic classification at the genus level revealed a predominance of *Acetobacter* across groups (Fig. 5A). The microbial composition of the control and PD groups was similar (Wald test,

Fig. 3 | Impact of consortium administration on PD pathophysiology in a *D. melanogaster* model. A Climbing assay at 10 days. **B** Climbing assay at 25 days. **C** Dopaminergic neurons positive for Tyrosine Hydroxylase enzyme, labeled with an antibody against the enzyme. The picture corresponds to a control fly fed with the consortium. **D** Analysis of dopaminergic neurons in the each group at 25 days. Statistical analysis was performed with two-way ANOVA followed by Tukey test (*$p < 0.05$, **$p < 0.01$, ***$p < 0.001$).
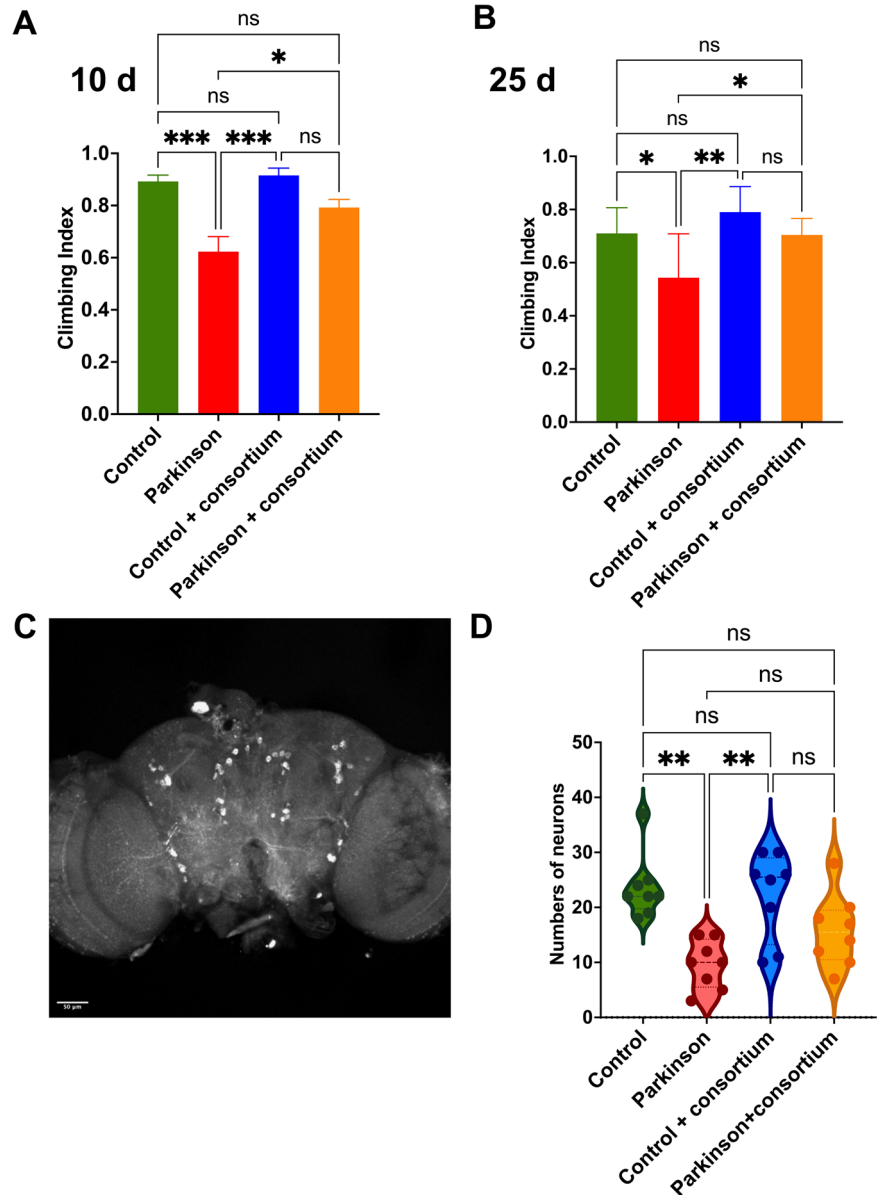
$p = 0.325$), whereas the microbiota of the C+ group differed significantly from that of controls (Wald test, $p = 0.045$). The PD+ group also displayed significant differences compared to both the PD and C+ groups (Wald test, $p = 0.007$ and $p = 0.049$, respectively), indicating that both the consortium and the disease model contributed to microbiome alterations. In particular, *Staphylococcus* spp. and *Corynebacterium* spp. were higher in the PD+ groups compared to control flies (One-Way ANOVA; $F = 41.592$; $p = 0.0475$ and One-Way ANOVA; $F = 142.279$; $p = 0.014$ respectively).

Shannon's diversity index of the PD+ group was significantly higher than the PD and control groups (One-Way ANOVA; Df: 3; F: 5.146; $p = 0.0285$); Fig. 5B. Therefore, treatment with the consortium in the PD group significantly increased the species diversity of the gut microbiome compared to the untreated group and control.

We finally conducted qPCR analysis with the 10 day-old fly's midguts to confirm these results. *L. brevis* G2 and *L. paracasei* M38 copy numbers in PD+ were significantly higher compared to the control group (One-Way ANOVA, Dunnett's multiple comparisons test, $n = 135$ per group, $p = 0.0007$ and $p = 0.0302$ for *L. brevis* G2 and *L. paracasei* M38, respectively) indicating these bacteria are found in the midgut of the flies (Fig. 6). However, their increased presence was lost by day 25 (Fig. 6).

Discussion

The computational models employed in this study helped predict microbial consortia with potential for neurometabolite production. By simulating metabolic fluxes and community interactions, SteadyCom enabled the identification of functionally diverse consortia, reducing the need for extensive empirical screening. Although semi-automated reconstructions lack the depth of fully curated GSMMs, they provided a practical framework to generate testable hypotheses. While results could be inaccurate due to these limitations, modeling microbial consortia suggested that metabolic cross-feeding increases neurometabolite production, implying that the availability of metabolic intermediates in the consortium increases GABA production.

There was a good agreement between model predictions and in vitro validation. In general, glucose predicted higher biomass production in these models, probably due to better curation of central metabolism. AGORA models predicted more GABA-producing bacteria than reconstructed models of this study, possibly due to improvements in this database allowing better predictions. Biomass and neurometabolite FVA showed different species abundance and neurometabolite production at suboptimal community growth rates, evidencing the trade-off between growth and production. This trade-off is reasonable, considering that the community uses
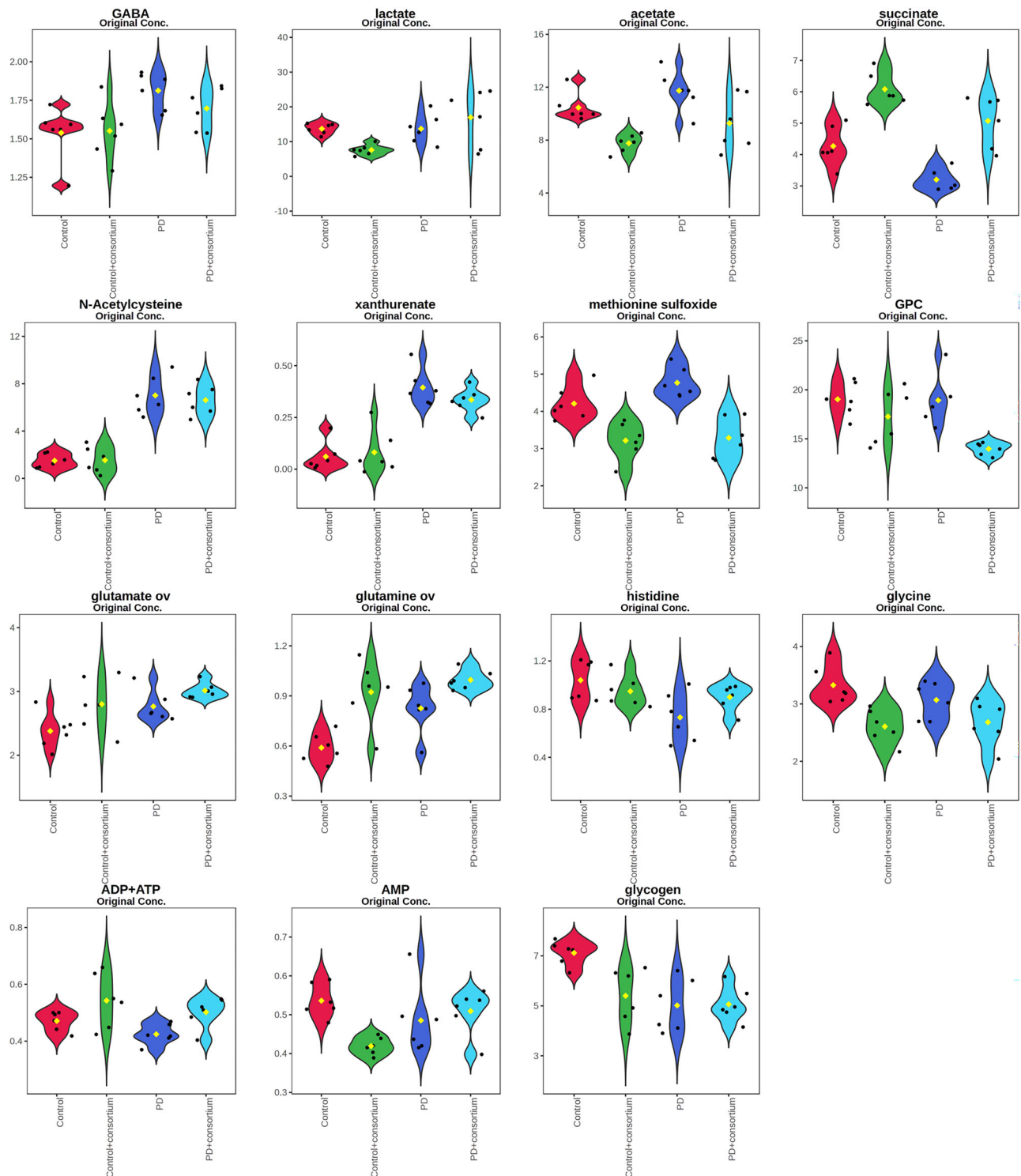
Fig. 4 | Distribution of metabolite concentrations among experimental groups. Violin plots illustrating the distribution and density of metabolite concentrations across experimental groups. Each dot represents an individual sample and the yellow dot indicates the mean value for each group. The width of each violin reflects the density of the data distribution. Statistical differences were evaluated using One-way ANOVA followed by Tukey's post-hoc test. *p*-values, FDR corrections and significant changes in pairwise comparisons are detailed in Supplementary Table 2.

its resources for biomass production, and GABA production is a secondary process associated with acid stress responses. Cross-feeding analysis also indicated which metabolites are essential in producing this molecule at the community level, where glutamate, acetate, and lactate appear to be directly related to GABA synthesis. In vitro GABA screening supported in silico predictions of single cultures and helped identify specific GABA-producing consortia that were evaluated later.

The PD model recapitulates most of the pathophysiology of the disease, including locomotive defects, reduction of dopaminergic neurons, and alterations in mitochondrial energy metabolism. Climbing ability in *D. melanogaster* declines with aging, being maximum and stable during the first 12−15 days and then decreasing progressively[42]. For the *D. melanogaster* PD model, the climbing test evidenced similar climbing scores as control flies in young flies but a premature loss of climbing ability compared
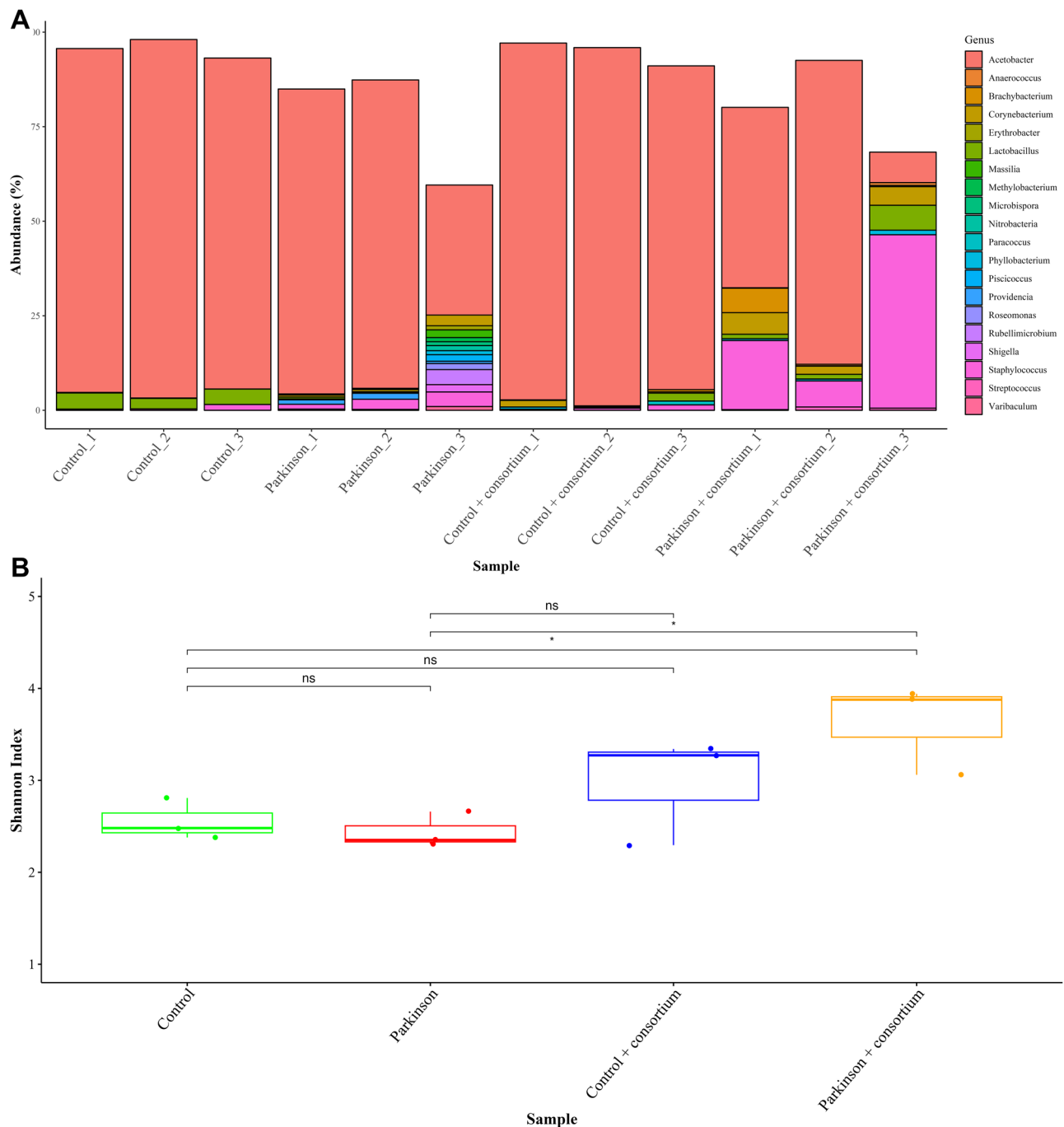
Fig. 5 | 16S rRNA-based analysis was used to determine microbial gut composition and diversity in the four Drosophila groups. A Stacked vertical bar charts illustrating species relative abundance. **B** Shannon diversity index for each group. Microbial diversity for PD+ group was statistically different from PD group (paired *t*-student test; $p = 0.028$).

to controls at 10 and 25 days. These results are coherent with other studies where *D. melanogaster* lines expressing α-synuclein A30P lose their climbing ability earlier than those expressing α-synuclein wild-type or A53T[39,46]. Interestingly, our findings suggest that the microbial consortium conferred a locomotor phenotypic rescue in the PD model since their climbing performance approached that of healthy control flies, indicating substantial mitigation of PD-related deficits. These results could be the product of the microbial synergic interactions in the consortium and the production of beneficial metabolites such as lactate, GABA, or other SCFAs.

Survival analysis in male flies showed that the consortium did not negatively affect fly longevity and even improved survival in control flies, indicating that the administration of human commensal bacteria is well

tolerated in this model. While male PD flies showed a trend toward reduced lifespan, consistent with prior reports of α-synuclein toxicity[40,41], this difference did not reach statistical significance, potentially due to environmental conditions that attenuate stress (e.g., abundant food, low density) or biological variability. The consortium consists of human commensal bacteria, which may not efficiently colonize other animal models.

Sex-specific differences in neurodegeneration models using *D. melanogaster* have been reported across various paradigms, particularly in Parkinson's disease (PD) models, where according to some studies females exhibit equal or greater resilience[47,48]. In our study, survival was assessed in males, which are often more susceptible to neurodegeneration, while
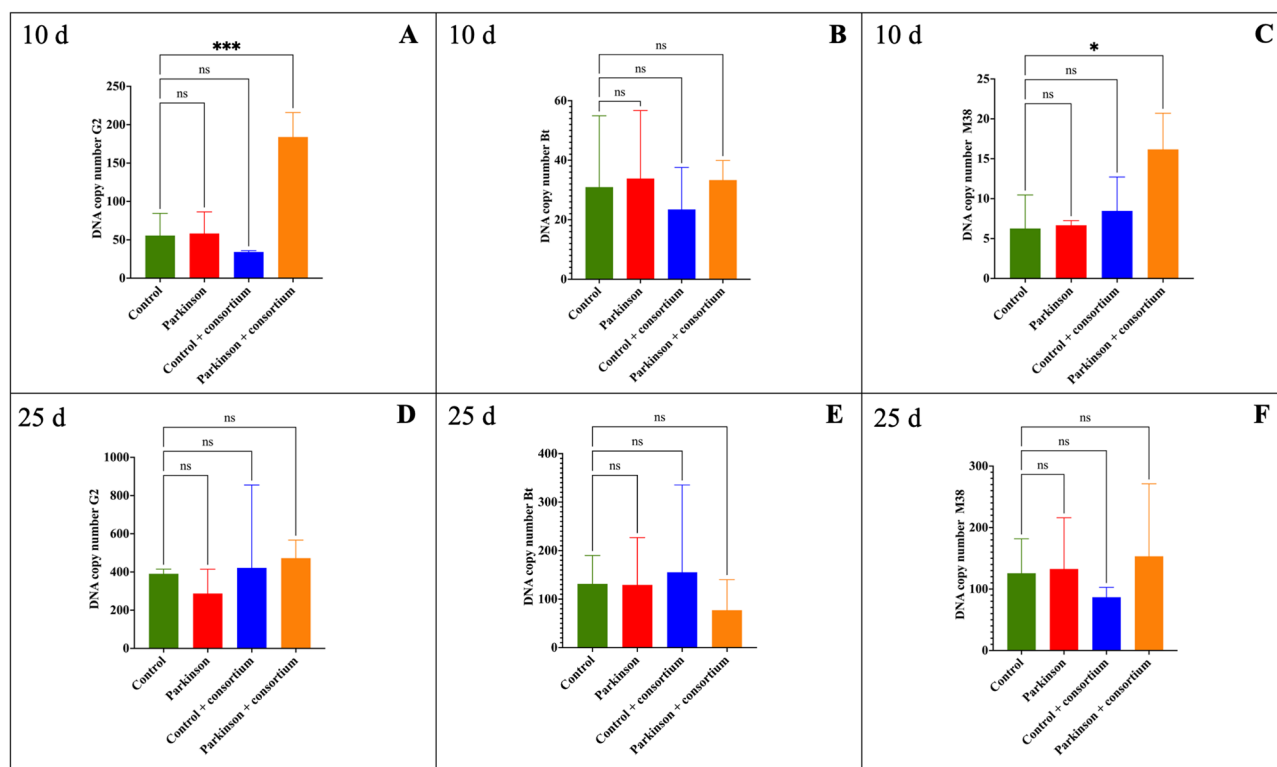
Fig. 6 | Genome copy number of consortium bacteria in experimental groups at 10 and 25 days. Statistical significance was evaluated compared to untreated control. **A** Genome copy numbers of *L. brevis* G2 at 10 days. **B** Genome copy number of *B. thetaiotaomicron* VPI 5482 at 10 days. **C** Genome copy number of *L. paracasei* M38 at 10 days. **D** Genome copy number of *L. brevis* G2 at 25 days. **E** Genome copy number of *B. thetaiotaomicron* VPI 5482 at 25 days. **F** Genome copy number of *L. paracasei* M38 at 25 days. (One way-ANOVA, Dunnett's multiple comparisons test *: $p < 0.05$, ***: $p < 0.001$, ns: not significant).

behavioral and metabolomic analyses were performed in females. This design limits direct comparisons across sexes.

Quantifying dopaminergic neurons in the fly brain provides a reliable readout for neurodegeneration in PD models[49]. Previous studies have evidenced that dopaminergic neuron loss in α-Syn mutants is age-dependent[40]. In this study, a reduction in dopaminergic neurons at 10 days of age showed no significant differences among the groups. Mohite et al.[41] also detected no signs of neurodegeneration at 10 days. However, substantial changes in dopaminergic neuron clusters were manifested on day 30, supporting our result. On day 25, dopaminergic degeneration was observed in PD flies compared to the control. Interestingly, the control and the PD groups receiving the consortium did not show differences between them and the control in the number of dopaminergic neurons, supporting a protection role of the consortium against neuronal degeneration. Although we cannot attribute this effect to a specific microbial metabolite, several mechanisms may be involved, including improved mitochondrial energy metabolism, modulation of neuroinflammation, or the action of neurometabolites produced or stabilized by the consortium. These findings are consistent with the behavioral improvements observed and support the hypothesis that microbial intervention can modulate PD-relevant neurobiological outcomes.

Neurodegenerative diseases are multifactorial disorders with unclear mechanisms for neuronal death[50]. These diseases are often characterized by mitochondrial dysfunction and increased levels of radical oxygen species[51]. PD has also been described as a metabolic syndrome, given its links to redox imbalance and impaired energy metabolism[52]. In our study, PCA showed a clear grouping of samples by phenotype, indicating that both the PD mutation and consortium administration significantly influenced brain metabolite profiles.

Metabolites related to energy production exhibited differential responses. Succinate levels were significantly increased in consortium-treated flies (both C+ and PD+), suggesting improved mitochondrial

function[53,54]. In contrast, ADP + ATP levels were not significantly altered by consortium administration, indicating that changes in high-energy phosphate compounds may not fully account for the observed neuroprotective effects. Similarly, although glucose metabolism disruptions have been associated with PD and other neurodegenerative diseases[52], glucose levels were not significantly modulated across experimental groups. Given that glucose is the primary energy source in the brain and is critical for nervous system function[55], these findings suggest that mitochondrial pathways rather than glycolytic flux may be the primary site of metabolic intervention.

Regarding amino acids, the low levels of essential amino acids such as histidine observed in PD flies are consistent with previous reports linking reduced histidine to increased clinical severity of PD[56]. However, this alteration was not restored by consortium administration. Additionally, glutamine levels remained elevated in both PD and C+ groups, suggesting that microbial exposure early in life influences amino acid metabolism independently of neurodegenerative processes. These persistent alterations indicate that amino acid metabolism is less responsive to microbial modulation under the tested conditions.

GABA levels were moderately elevated in PD flies compared to controls but were not significantly modulated by consortium administration. This suggests that neurotransmitter-related pathways may not be the primary targets of the observed neuroprotective effects.

Metabolites related to oxidative stress showed more robust responses. Methionine sulfoxide levels, elevated in PD flies, were significantly reduced in PD+ flies, suggesting improved redox homeostasis and partial restoration of the methionine sulfoxide reductase (Msr) system function[57]. Given the role of methionine oxidation in α-synuclein aggregation[58–60], these results suggest that consortium administration may mitigate oxidative stress-related protein aggregation. Additionally, GPC levels, typically increased in PD, were reduced following treatment, further supporting the restoration of redox balance. However, other oxidative stress-related metabolites, such as N-acetylcysteine and xanthurenate, remained elevated
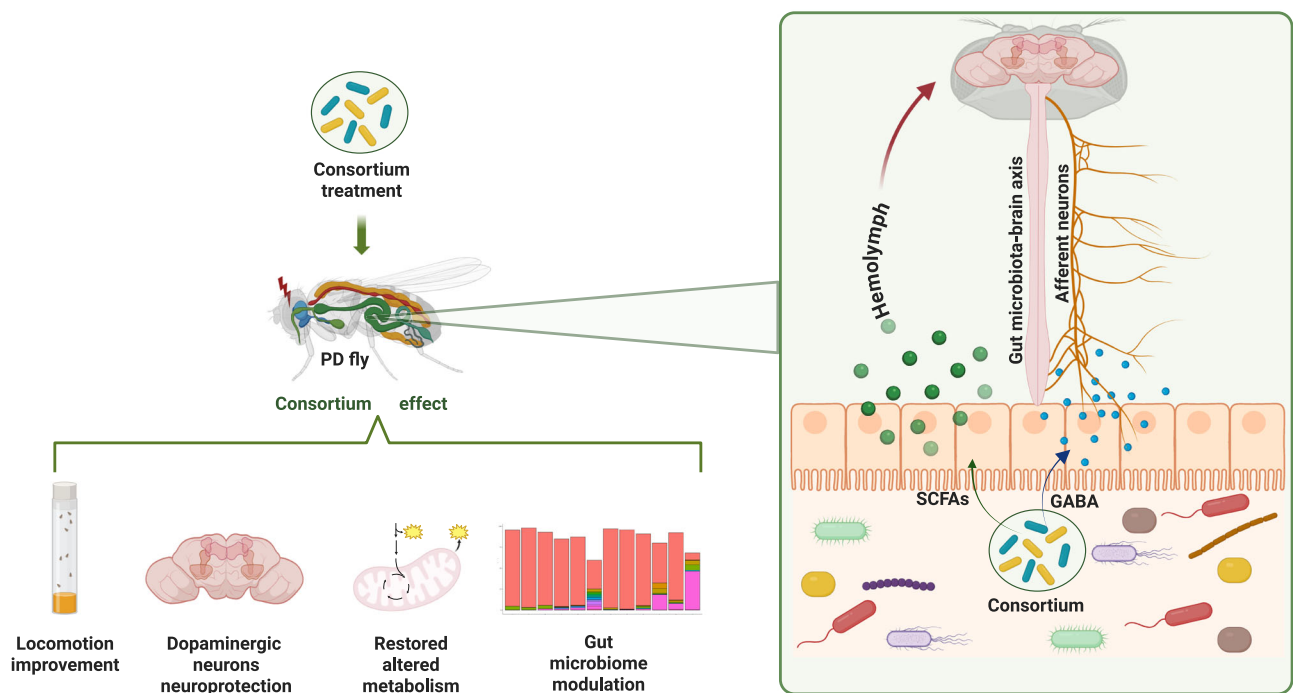
Fig. 7 | Proposed mechanisms of action of microbial consortium in *D. melanogaster* PD model. This figure presents potential interactions between the administered microbial consortium and changes in brain physiology in the context of Parkinson's disease (PD). It includes proposed pathways by which microbial metabolites, such as GABA, lactate or other SCFAs might contribute to neuroprotection, potentially influencing inflammation and dopaminergic signaling.

in PD and PD+ flies, indicating persistent redox imbalance in certain pathways.

Finally, metabolites related to energy reserves and purine metabolism showed selective alterations. AMP and glycogen were significantly reduced in C+ flies compared to controls, and glycogen was also lower in PD flies relative to controls. These results suggest alterations in energy storage and turnover linked to both disease and microbial exposure. Overall, these findings indicate that consortium administration partially restores metabolic balance in PD flies, affecting pathways involved in energy metabolism, oxidative stress, and neurotransmission. This supports the idea that metabolite-mediated modulation of host physiology may contribute to the neuroprotective effects observed.

Several studies have shown that the gut microbiome is altered in patients with PD compared to healthy individuals[25]. Gut microbiome imbalance has been hypothesized to be responsible for many gastrointestinal disorders observed in this disease[61]. Moreover, microbiome dysbiosis in PD has been proposed to play a role in non-gastrointestinal symptoms, specifically those related to the microbiome-gut-brain axis[62]. In this study, the *Acetobacter* abundance was slightly higher in the PD group than in the control, and a higher *Lactobacillus* proportion was shown compared to the control. A higher abundance of acetic acid bacteria in PD flies (*park*[25] mutants), and a higher proportion of lactic acid bacteria in control flies have been reported[63], with the latter being concordant with our observations. The consortium administration reduced *Acetobacter* abundance, which was more noticeable in the PD group. The consortium significantly increased the gut microbiome diversity in the control and PD groups concerning the untreated groups. The increased diversity was more noticeable in the PD group with treatment, as the disease tends to reduce the diversity of the gut microbiome compared to the healthy group[64]. The increase in *Staphylococcus* in the PD and especially PD+ groups is remarkable, and could be explained by the genetic model being more easily colonized by this genus and the consortium creating a niche favorable for these bacteria.

qPCR results detected *L. brevis* and *L. paracasei* in PD+ group suggest that early administration enables midgut colonization during larval development. Their presence also suggests that their metabolic activity partly explains the improvement of PD pathophysiology. In contrast, *B. thetaiotaomicron* DNA was not identified in any group, probably due to its more fastidious and narrow growth inside the fly midgut, characterized by colder temperature (25 °C) and higher oxygen concentration. Despite the lack of *B. thetaiotaomicron* colonization, the G2M38 sub-consortium produces similar amounts of GABA, as evidenced by our in vitro data (Supplementary Fig. 4). However, this work did not evaluate how much GABA is being produced in vivo by the consortium. While we did not quantify GABA in vivo or perform metabolic tracing, our results indicate that early-life exposure to *Lactobacillus* strains can modulate gut composition and contribute to improved PD-related phenotypes. These findings support the feasibility of targeting the microbiota–gut–brain axis using tailored consortia.

We propose the following mechanisms of action for the consortium in the PD model. The G2BtM38 microbial consortium showed a neuroprotective effect in a *D. melanogaster* PD model, as evidenced by improved locomotion and metabolomic profile, and partially preserved dopaminergic neurons (Fig. 7). *D. melanogaster* possesses a structurally defined blood-brain barrier (BBB) formed by subperineurial glial cells, which restrict paracellular diffusion and regulate metabolite entry into the brain. Although simpler than its vertebrate counterpart, the *Drosophila* BBB performs an analogous protective role, maintaining neural homeostasis and shielding the brain from systemic fluctuations. In this context, it is unlikely that microbial GABA, even if produced in the gut or hemolymph, could cross the BBB to exert a direct neural effect[65,66]. However, TCA intermediates and neurotransmitter precursors generated by microbial metabolism—such as glutamate or aspartate—may enter the brain through regulated transport[67], potentially influencing neuronal function indirectly. For instance, microbial GABA may be catabolized in the gut via the GABA shunt, replenishing the TCA cycle and contributing to energy balance[68]. Additionally, SCFAs, lactate or even succinate could enter systemic circulation and affect host metabolism with a neuroprotective effect[69–71]. Moreover, the consortium increased gut microbial diversity, which may contribute to microbiota resilience and functional plasticity, as well as metabolic changes impacting

brain responses. These changes likely act in combination to support host homeostasis and mitigate PD-related decline[71,72].

Finally, this study has several limitations that should be acknowledged. First, while our in silico approach efficiently identified consortia with neurometabolite production potential, the metabolic reconstructions used were semi-automated and not manually curated. As such, model predictions —particularly for metabolite fluxes—may be affected by incomplete pathway annotations, imprecise stoichiometries, or generic growth conditions that do not fully reflect the fly gut environment. Second, although the selected consortium produced GABA and SCFAs in vitro, we could not directly confirm their production or availability in vivo. GABA was not consistently elevated in fly brains, and we did not apply metabolic tracing or labeling approaches to determine microbial contribution to host metabolites. Thus, the causal link between microbial metabolite production and neuroprotection remains putative. Additionally, our metabolomic analysis was based on whole-head samples, which may have masked localized metabolite changes in vulnerable dopaminergic neurons. Future studies should consider targeted metabolomic profiling to resolve this limitation. Third, the colonization capacity of the consortium was only partial and transient. While *L. brevis* and *L. paracasei* established in the fly midgut early in life, *B. thetaiotaomicron* was not detected—likely due to its fastidious growth requirements and poor adaptation to the fly gut conditions (e.g., higher oxygen levels, lower temperature). This incomplete implantation may have limited the in vivo production of some target metabolites. Moreover, we did not evaluate the contribution of each bacterial strain independently, nor the effect of dosage or administration timing. These factors may influence colonization dynamics and metabolic output and should be considered.

A further limitation involves the use of different sexes across experimental endpoints. Survival was assessed in males, while behavioral, metabolomic, and microbiome analyses were conducted in females. This design reflects practical constraints and the aim to minimize variability by using one sex for core assays. Female flies were prioritized in these assays to improve reproducibility and reduce variability. However, we acknowledge that this sex-specific allocation was not based on a fully systematic rationale at the time of study design. As a result, the comparison of survival with other endpoints is limited, and the absence of sex as an experimental variable reduces the generalizability of our findings.

As final remarks, this study demonstrates the feasibility of rationally designing microbial consortia with neurometabolite-producing potential using metabolic modeling. The selected consortium modulated gut microbial diversity, partially preserved locomotor function and dopaminergic neurons, and restored key metabolic alterations in PD flies—despite lack of direct confirmation of in vivo GABA production or uptake. These results support the potential of early-life microbial interventions to modulate host neurophysiology via gut–brain axis mechanisms, highlighting the importance of metabolic cross-feeding and strain compatibility in shaping functional outcomes. While *D. melanogaster* offers powerful tools for mechanistic exploration, extrapolation to human physiology must be done with caution due to species-specific differences in gut architecture, immunity, and neural complexity. Future studies should refine strain-level contributions, integrate metabolic tracing, and evaluate sex-specific and host-specific responses to microbial therapies in neurodegeneration.

Methods
Genome sequencing and metabolic models
Supplementary Table 1 shows the microorganisms and metabolic reconstructions used in this study. For genome sequencing, the total DNA of isolated bacteria pellets was extracted using the phenol-chloroform protocol previously described[73]. Total DNA concentration was quantified using a Nano-Quant plate in a Tecan Infinite M200 Pro microplate reader by measuring the absorbance at OD_{260}. Libraries and subsequent DNA sequencing of the bacteria samples were performed by MicrobesNG (Birmingham, U.K.). Illumina MiSeq platform with 250 bp paired-end sequencing reads was used. Illumina adapter TruSeq3-PE sequences and

low-quality bases were trimmed from raw fastq reads using Trimmomatic v0.36[74]. Trimmed reads data quality was evaluated with FastQC v0.11.5 and was de novo assembled using SPAdes v3.13.0 with default parameters[75]. The reads obtained were assembled and annotated with SPADES and PROKKA from KBase[76]. Subsequently, draft metabolic reconstructions of these genomes were automatically generated with ModelSEED of KBase[76]. The models were cured automatically by gap-filling using the Gapfill Metabolic Model tool from KBase[76] and manually using reported information and previously published GSMMs.

Computational optimization of bacterial consortia producing GABA and butyrate
An initial in silico screening of neurometabolic-producing consortia using metabolic reconstructions was performed. Monoculture and consortia flux simulations were done in MATLAB 2022a using the COBRA Toolbox v3.0[77] and GUROBI v9.0.3 optimizer. Metabolic reconstructions from genomes used in this study, including GABA- and butyrate-producing bacteria GSMMs, were obtained from AGORA v3.0[78] (Supplementary Table 1). The modified version of culture media ZMB (mZMB)[79] with glucose or inulin as the carbon source was used for growth simulations. The consortia were simulated using the SteadyCom algorithm from the COBRA Toolbox, which allows us to obtain the maximum community steady-state growth rate and flux distribution at this optimum rate[80]. In addition, SteadyCom calculates the relative abundance of each species from the consortia and seeks to determine cross-feeding between the consortia members. Each designed consortium had at least one bacterium from the following categories: primary fermenters (*Bifidobacterium*, *Bacteroides*), secondary fermenters (*Lactobacillus*), and GABA or butyrate producers. The final consortium comprised a maximum of five species to reduce the experimental variability in the following stages.

Strains and culture media monoculture and co-culture assays
The microorganisms of Supplementary Table 1 were cultured in Reinforced Clostridial Medium (RCM, Becton-Dickinson, Franklin Lakes, NJ) or de Man Rogosa and Sharpe broth (MRS, Becton-Dickinson, Franklin Lakes, NJ), supplemented with 1 g/L and 0.5 g/L of L-cysteine (Loba Chemie, India) respectively. Bacteria were cultured from a −80 °C stock in the corresponding complex medium under anaerobic conditions. Then, the bacteria were incubated at 37 °C for 48 h in anaerobic jars (Medica-Tec, Chile) with anaerobic packs (Gaspak EM, Becton-Dickinson, Franklin Lakes, NJ, USA). The monoculture assay was performed in 96-well plates on mZMB medium with glucose (20 g/L) or inulin (1 g/L) as a carbon source under sterile conditions. Microorganisms were inoculated at 5% v/v, and wells were covered with a mineral oil layer (20 µL). The strains were cultured in triplicates at 37 °C for 48 h in an anaerobic chamber (Sheldon Manufacturing INC, Bactronez-Anaerobic Chamber Workstation, Cornelius, OR, USA). The optical density was measured at OD_{620nm} on a Tecan F50 spectrophotometer (TecanTrading AG, Infinite F50, Mannedorf, Switzerland), which was located inside the chamber every 30 min with a 5 s shaking before measurement. Co-culture was carried out the same way as monoculture, and bacteria forming a consortium were added in equal proportions to the inoculum.

GABA production screening
A screening for GABA production was performed by thin-layer chromatography (TLC)[17]. The assay was performed in triplicate on 96-well plates, and each bacterium was cultured (5% v/v) in the respective complex media, mZMB medium with glucose (20 g/L), and mYCFA medium was used[81]. These media were supplemented with monosodium glutamate (10 g/L) to induce GABA production. The plate wells were covered with a mineral oil layer (20 µL), and the strains were cultured at 37 °C in anaerobic patch jars for 48 h. OD_{620nm} was measured in a spectrophotometer (Tecan, Mod. Infinite® 200 PRO, Switzerland). The supernatant was stored at −20 °C for further analysis. Similarly, co-cultures were evaluated in mZMB medium with inulin (1% w/v) with and without monosodium glutamate (1% w/v),

and the consortium was inoculated at 5% (v/v), where each species was in equal proportion. TLC was performed in F-60 silica plates (Merck, Germany), using a running buffer (N-butanol, acetic acid with 99% purity, and water for chromatography in the proportions 4:1:1). Two μL were taken from each sample supernatant sample. To develop the chromatogram, the silica plate was dried, placed in a developing solution (0.8% (w/v) ninhydrin and distilled water as solvent), and heated at 100°C for 10 min or until the spots were visible.

Batch bioreactor cultivation

Batch experiments were conducted in 250 mL bioreactors connected to a MyControl system (Mini-bio Applikon Biotechnology, Netherlands) in duplicate for the consortia that exhibited the highest GABA production. The optimized mZMB culture medium was used, supplemented with 10 g/L inulin, 0.5 g/L L-cysteine, and 0.1% (w/v) monosodium glutamate. The strains of a given consortium were inoculated at an initial OD_{620nm} of 1, and the bioreactor was maintained at 37 °C, pH 5.5, at 90 rpm agitation in an anaerobic environment by nitrogen injection (99.99% purity grade) to simulate proximal colon conditions[82]. Samples were taken every 2 h for 1 day and stored at −20 °C for further analysis.

Substrate consumption

TLC was performed from bacterial supernatants at 0 h, 12 h, and at the end of the fermentation time. Briefly, supernatant samples (2 μl) were loaded on F-60 silica plates (Merck, Germany). The reactor culture media was used as the control, and carbohydrate standards were prepared (1 g/L). The TLC sheets were developed twice with a running solution of n-butanol, acetic acid, and water at a 2:1:1 (v/v) ratio. Staining solution (0.5% α-naphthol, 5% H_2SO_4, and molecular grade ethanol as solvent) was added for band visualization, followed by air drying at 100 °C.

GABA quantification

GABA concentration was quantified using TLC and the method of Watchararparpaiboon et al.[83]. Briefly, the mixture (0.2 M borate buffer, 0.2 mL: 6% phenol reagent, 1 mL) was added to the supernatants (0.1 mL). Subsequently, 0.4 mL of 7.5% sodium hypochlorite was added, and the samples were brought to 100 °C in a thermoregulated bath for 10 min. They were then immediately cooled in an ice-water bath for 5 min, and the optical density was measured at 630 nm. The calibration curve with GABA standard was prepared in a concentration range of 0-4 g/L, which yielded a determination coefficient (R^2) of 0.99 and was used to determine the concentration of GABA in the samples.

SCFA quantification

The concentration of acetate, butyrate, lactate, propionate, and succinate was quantified by high-performance liquid chromatography (HPLC) using a Lachrom L-700 liquid chromatograph (Merck-Hitachi, Japan) equipped with a UV detector at 210 nm. On the Aminex HPX-87H ion exclusion column (300 mm, 7.8 mm; Bio-Rad, Hercules CA, USA), samples were eluted with H_2SO_4 (5 mM) at a flow rate of 0.45 mL/min at 35 °C for 35 min. Acetic, butyric, lactic, propionic, and succinic acid standards of known concentrations were used for column calibration (Sigma-Aldrich, St. Louis, MO, USA). Thirty microliters of each sample were injected and analyzed in duplicate. Sample detection was carried out by comparing retention times with standards. Each standard ranged in concentration from 0.155 mg/mL to 20 g/L. Data analysis was performed with Multi-HSM Manager software (Hitachi, Japan).

Determination of relative bacterial abundances in the consortia

Total DNA extraction from cell pellets was performed using an adaptation of the phenol-chloroform-isoamyl alcohol protocol[73]. DNA was quantified using a NanoQuant plate in a Tecan Infinite M200 Pro microplate reader and diluted to 10 ng/μl. Bacterial absolute and relative abundances were determined by qPCR, using a set of species-specific primers based on unique gene sequences present in each bacterium (Supplementary Table 3). The reagent concentrations used were those of the kit SensiFAST™ SYBR® No-ROX Kit (Bioline, USA) with annealing temperatures of 60 °C. Reactions were performed in triplicates.

D. melanogaster strains and husbandry

Flies and crosses were raised on standard *D. melanogaster* food at 25 °C in 12 h light/dark cycles. Fly stocks used in the study were *elav*-GAL4 (Bloomington 458), UAS-α-*Syn* (A30P) (Bloomington 8147), and w^{1118}(CS) (donation). The *elav*-GAL4 line (called a driver), expressing the GAL4 transcription factor under a neuronal promoter (*elav*), was crossed to flies from UAS-α-*Syn* line expressing the A30P mutant of the human α−synuclein under UAS control (also called responder) for the PD group. For the control group, w^{1118}(CS) was crossed with *elav*-GAL4.

Generation of germ-free flies

Germ-free flies were generated according to a previously described protocol that was modified[36]. The eggs were washed with sodium hypochlorite (0.5% v/v) for 5 min and three 5-min washes with distilled water under sterile conditions. For control and PD groups that did not receive consortium, axenic eggs were transferred to bottles with standard sterile food previously left overnight in contact with control flies. In contrast, the axenic eggs were transferred in bottles with sterile standard food for the control and PD groups that received the consortium. However, these bottles were not exposed to control flies but were inoculated with the consortium every 48 h for 10 days from the larval stage until hatching. A standard diet was composed of 11 g/L agar, 100 g/L yeast extract, 10 g/L wheat flour, 50 g/L corn flour, 80 g/L glucose, 0.6% (v/v) propionic acid and 1.2% (v/v) methyl parahydroxybenzoate (Nipagin) as antifungal. A dose of 200 μl of the bacterial consortium (10^8 cells/ml each bacterium) was added, and larvae were transferred to standard food (with or without consortium) every 2 days.

Consortium culture

Consortium bacteria were cultured (10% v/v inoculum) in their respective complex media for 48 h at 37 °C under anaerobic conditions. *Lactobacillus* strains were cultured in MRS-cys and *Bacteroides* strain on RCM-cys. The cultures were centrifuged at 8000 x *g* for 2 min, and the pellets were resuspended in sterile phosphate-buffered saline (PBS) supplemented with inulin (1% v/v) as carbon source and monosodium glutamate (0.1% v/v) to induce GABA production. The average growth of single culture bacteria (OD_{620}) was 0.5, 2.0, and 2.6 for *B. thetaiotaomicron* VPI 5482, *L. brevis* G2, and *L. paracasei* M38, respectively and was 5.7 for the selected consortium. For inoculation, 300 μL of the bacterial consortium culture was administered to each group.

Climbing Assay

The climbing assay was performed based on the negative geotactic behavior of flies[42]. Groups of 135 1 day-old female flies were collected for each condition under brief CO_2 exposure, placed in fresh food vials in groups of 35 per/vial, and tested at 10 or 25 days. Before the test, flies were kept at 25 °C for 15 min on the bench to acclimate to the assay environmental conditions. A counter-current apparatus with six tubes in the lower frame and five in the upper part was used for the test[84]. Each group of flies was placed in the first apparatus (1.5 cm diameter and 10 cm height) and gently tapped to the bottom. After 10 s, the upper frame was moved to the right, and the flies that passed in the upper tubes for 30 s were transferred to the following lower tubes by gently tapping. This procedure was repeated five times. The climbing index was calculated using the following formula for each genotype[84].

$$CI = \left[(\#F5 \times 5) + (\#F4 \times 4) + (\#F3 \times 3) + (\#F2 \times 2) + (\#F1 \times 1) + \frac{\#F0 \times 0}{\#FT} \right]$$

$$(1)$$

#Fn is the number of flies in the tube, "n" (0 in the initial tube and 5 in the last tube), and #FT is the total number of flies.

Survival assays

Survival assays were performed to evaluate half-life. Experiments were carried out with 60 one-day-old male flies of the F1 generation for each genotype. Flies were transferred to a new vial every two days, and the number of live flies was recorded. Flies were maintained at 25 °C under a 12 h light/dark cycle. The percentage of survival was calculated at the end of the experiments.

Immunofluorescence and imaging

Dopaminergic neurons were quantified by immunofluorescence. 10 and 25 day-old adult female flies were used, where 10 brains were imaged per experimental group. Flies were anesthetized with CO_2, and their brains were dissected in cold PBS 1X and fixed with 4% paraformaldehyde at 25 °C for 15 min. The brains were washed with PBS 1X supplemented with triton (0.3%) (PBST) at 25 °C for 5 min. The brains were blocked with PBST containing 1% normal goat serum at 25 °C for 1 h. Tyrosine hydroxylase (TH) enzyme was applied as a marker for DA neurons. Brain samples were incubated with the primary antibody (Rabbit anti-TH, Merck, Cat# AB152) and diluted in the blocking solution (PBST containing 1% normal goat serum; 1:500) at 4 °C overnight. Next, samples were washed four times with PBST incubated with the secondary antibody (Rabbit fit C, Jackson InmunoResearch, USA, catalog number: 111-095-003) and diluted in blocking solution (1:300) at 25 °C for 2 h[85]. Brains were washed and mounted in VECTASHIELD Mounting Medium[86]. Confocal images were taken with an Olympus FV1000 confocal microscope (Shinjuku, Tokyo, Japan), and the number of total dopaminergic neurons was determined using ImageJ software[87].

Metabolite extraction

Head metabolite extraction was performed as previously described[88]. Six samples of 10 day-old flies were prepared for each experimental group, containing 50 heads of female flies each. Heads were frozen by immersion in liquid nitrogen. Then, 240 μL of cold methanol and 48 μL of cold Milli-Q water were added to each tube and incubated for 5 min. The heads were then homogenized with a small mortar for 60 s vortexed, 120 μL of cold $CHCl_3$ and 120 μL of cold Milli-Q water were added and vortexed again. The samples were then incubated at 4 °C for 15 min and centrifuged at 10,000 x g at 4 °C for 15 min. After this, two phases were formed: an aqueous phase at the top with polar metabolites and a lower lipophilic phase with non-polar metabolites. The aqueous phase was frozen with liquid nitrogen and stored at −80 °C until further use.

NMR-1H Analysis

Aqueous extracts were placed on ice and resuspended in 550 μl of NMR buffer (20 mM NNaP, 20 μM (trimethylsilyl)-2,2',3,3'-tetraduteropropionic acid (TSP), pH = 7.4 in D_2O). The supernatant was transferred to a 5 mm NMR tube. NMR spectra of the extracts were recorded at 27 °C on a 600 MHz Bruker NMR spectrometer equipped with a 5 mm TCI cryoprobe. One-dimensional 1H-NMR NOESY spectra were acquired with 360 free induction decays (FIDs) for the aqueous extracts. 64,000 data points were digitalized over a spectral width of 30 ppm for extract spectra. A 3 s relaxation delay was included between FIDs, and water presaturation was applied. The FID values were multiplied by an exponential function with a 0.5 Hz line broadening factor. Total Correlation Spectroscopy (TOCSY) and multiplicity Heteronuclear Single Quantum Correlation (HSQC) were performed for representative samples for signal assignment. 256-512 t1 increments were used for each experiment, and 32−96 transients were collected.

Metabolite assignment and quantification

Metabolite identification and assignment were performed with the help of databases (Amix, HMBD, and Biological Magnetic Resonance Data Bank),

literature values, and information from 2D NMR experiments. For metabolite quantification, spectra were automatically integrated at selected regions with MestreNova. For a better comparison between extract samples, integration values were normalized to total intensity to minimize the variability generated by the extraction procedure.

Multivariate analysis of metabolites

Multivariate and univariate statistical analyses were primarily performed using the MetaboAnalystR 4.0 platform[89], complemented by exploratory multivariate analyses in SIMCA-P 16.0 (Umetrics, Sweden). Principal Component Analysis (PCA) was used for an initial overview of sample distribution and identification of outliers. Supervised Partial Least Squares Discriminant Analysis (PLS-DA) models were generated to evaluate class separation, with model quality assessed through R^2 and Q^2 values. For visualization of global metabolic patterns, log10-transformed data were analyzed using hierarchical clustering in MetaboAnalyst, applying Euclidean distance and Ward's linkage methods to generate heatmaps illustrating group-specific metabolic profiles. Univariate analysis was conducted using One-way ANOVA to identify metabolites with significant differences among groups. Pairwise comparisons were performed with Tukey's post-hoc test, and correction for multiple comparisons was applied using the False Discovery Rate (FDR) method. Statistical significance was considered at $p < 0.05$.

16S rRNA sequencing and analysis

DNA gut samples of *D. melanogaster* were prepared for 16S rRNA gene sequencing to evaluate gut microbiome composition in the four experimental groups. Sequencing libraries were prepared by extracting DNA from the midgut of 10 day-old female flies using the Zymo Quick-DNA fecal/soil microbe kit, following manufacture protocol (D6011, Zymo, Irvine, CA). A pool of 15 midgut samples was collected in triplicate per group. DNA samples were sent for sequencing to Molecular Research (www.mrdnalab.com, Shallowater, TX, USA). DNA was amplified using the 515 F/806 R (515 F:5′-GTGYCAGCMGCCGCGGGGTAA3′, 806 R:5′ GGACTACNVGGGGGTWTCTAAT-3′) primers, which recognize the V4 region of bacterial 16S ribosomal DNA. Sequencing was performed on an Illumina MiSeq sequencer following the manufacturer's guidelines (Illumina, USA). Sequenced reads were analyzed using QIIME2[90] and R software[91]. Reads were trimmed based on quality scores, denoised, and dereplicated using DADA2[92], eliminating chimeras and filtering the reads to a minimum length of 240 nt. Taxonomic classification was assigned using the GreenGenes 13.8 database[93] trained for the classify-sklearn classifier. Taxonomic annotation results were exported for Operational Taxonomic Units (OTUs) and converted to Phyloseq format in R. Relative abundance of genera and species was plotted; differential abundance analysis was performed for the different conditions with Deseq[94] using the Wald test. Finally, Shannon diversities were calculated and plotted for significance using a t-test to compare significant differences between conditions.

Consortium identification on *D. melanogaster* gut microbiome

The consortium species in the gut microbiome of 10- and 25 day-old females for each condition was identified by qPCR according to the methodology described in section 2.9. Fifteen midguts were dissected in triplicate for the 10 day-old groups, and 30 were dissected in triplicate for the 25 day-old groups per group.

Statistical analysis

Statistical analysis was performed with PRISM v 9.4.1 (GraphPad, La Jolla, CA), using One-Way and Two-Way ANOVA, with post-hoc Tukey's or Dunnett's tests to determine differences between each condition or group with a confidence level of 95%.

Data availability

Data is provided in the supplementary information files.

Article

References

1. Tamburini, S., Shen, N., Wu, H. C. & Clemente, J. C. The microbiome in early life: implications for health outcomes. *Nat. Med.* **22**, 713–722, https://doi.org/10.1038/nm.4142 (2016).
2. Duvallet, C., Gibbons, S., Gurry, T., Irizarr,y R., Alm, E. Meta analysis of microbiome studies identifies shared and disease-specific patterns. *Nat. Commun.* **8**, 1784 (2017).
3. Kamada, N., Seo, S.-U., Chen, G. Y. & Núñez, G. Role of the gut microbiota in immunity and inflammatory disease. *Nat. Rev. Immunol.* **13**, 321–335 (2013).
4. Sun, P. et al. Gut microbiota regulation and their implication in the development of neurodegenerative disease. *Microorganisms* **9**, 2281 (2021).
5. Cryan, J. F. et al. The microbiota-gut-brain axis. *Physiol. Rev.* **99**, 1877–2013, (2019).
6. Boeckxstaens, G. The clinical importance of the anti-inflammatory vagovagal reflex. *Handb Clin. Neurol.* **117**, 119–134 (2013).
7. Bonaz, B., Sinniger, V. & Pellissier, S. Anti-inflammatory properties of the vagus nerve: potential therapeutic implications of vagus nerve stimulation. *J. Physiol.* **594**, 5781–5790 (2016).
8. Sudo, N. et al. Postnatal microbial colonization programs the hypothalamic-pituitary-adrenal system for stress response in mice. *J. Physiol.* **558**, 263–275 (2004).
9. Fung, T. C., Olson, C. A. & Hsiao, E. Y. Interactions between the microbiota, immune and nervous systems in health and disease. *Nat. Neurosci.* **20**, 145–155 (2017).
10. Zhang, Q. et al. Accelerated dysbiosis of gut microbiota during aggravation of DSS-induced colitis by a butyrate-producing bacterium. *Sci. Rep.* **6**, 27572 (2016).
11. Li, H. et al. Sodium butyrate exerts neuroprotective effects by restoring the blood-brain barrier in traumatic brain injury mice. *Brain Res.* **1642**, 70–78 (2016).
12. Liu, J. et al. Sodium butyrate exerts protective effect against Parkinson's disease in mice via stimulation of glucagon like peptide-1. *J. Neurol. Sci.* **381**, 176–181 (2017).
13. Wu, X. et al. Histone deacetylase inhibitors up-regulate astrocyte GDNF and BDNF gene transcription and protect dopaminergic neurons. *Int. J. Neuropsychopharmacol.* **11**, 1123–1134 (2008).
14. Strandwitz, P. Neurotransmitter modulation by the gut microbiota. *Brain Res.* **1693**, 128–133 (2018).
15. Asano, Y. et al. Critical role of gut microbiota in the production of biologically active, free catecholamines in the gut lumen of mice. *Am. J. Physiol. Gastrointest Liver Physiol.* **303**, G1288–G1295 (2012).
16. Petra, A. I. et al. Gut-microbiota-brain axis and its effect on neuropsychiatric disorders with suspected immune dysregulation. *Clin. Ther.* **37**, 984–995 (2015).
17. Yunes, R. A. et al. GABA production and structure of gadB/gadC genes in Lactobacillus and Bifidobacterium strains from human microbiota. *Anaerobe* **42**, 197–204 (2016).
18. Feehily, C. & Karatzas, K. A. G. Role of glutamate metabolism in bacterial responses towards acid and other stresses. *J. Appl. Microbiol.* **114**, 11–24 (2013).
19. Strandwitz, P. et al. GABA-modulating bacteria of the human gut microbiota. *Nat. Microbiol.* **4**, 396–403 (2019).
20. Bravo, J. A. et al. Ingestion of Lactobacillus strain regulates emotional behavior and central GABA receptor expression in a mouse via the vagus nerve. *Proc. Natl. Acad. Sci. USA* **108**, 16050–16055 (2011).
21. Duman, R. S., Sanacora, G. & Krystal, J. H. Altered connectivity in depression: GABA and glutamate neurotransmitter deficits and reversal by novel treatments. *Neuron* **102**, 75–90 (2019).
22. Nuss, P. Anxiety disorders and GABA neurotransmission: a disturbance of modulation. *Neuropsychiatr. Dis. Treat.* **11**, 165–175 (2015).
23. Patterson, E. et al. Gamma-aminobutyric acid-producing lactobacilli positively affect metabolism and depressive-like behaviour in a mouse model of metabolic syndrome. *Sci. Rep.* **9**, 1–15 (2019).
24. Luscher, B., Shen, Q. & Sahir, N. The GABAergic deficit hypothesis of major depressive disorder. *Mol. Psychiatry* **16**, 383–406 (2011).
25. Baldini, F. et al. Parkinson's disease-associated alterations of the gut microbiome predict disease-relevant changes in metabolic functions. *BMC Biol.* **18**, 62 (2020).
26. Clos-Garcia, M. et al. Gut microbiome and serum metabolome analyses identify molecular biomarkers and altered glutamate metabolism in fibromyalgia. *EBioMedicine* **46**, 499–511 (2019).
27. Urrutia, A. et al. Bacterially produced metabolites protect C. elegans neurons from degeneration. *PLoS Biol.* **18**, e3000638 (2020).
28. O'Hagan, C. et al. Long-term multi-species Lactobacillus and Bifidobacterium dietary supplement enhances memory and changes regional brain metabolites in middle-aged rats. *Neurobiol. Learn. Mem.* **144**, 36–47 (2017).
29. Omotosho, A. O. et al. Parkinson's disease: are gut microbes involved? *Brain Behav.* **13**, e3130 (2023).
30. Scheperjans, F. et al. Gut microbiota are related to Parkinson's disease and clinical phenotype. *Mov. Dis.* **30**, 350–358(2015).
31. Gerhardt, S. & Mohajeri, M. H. Changes of colonic bacterial composition in parkinson's disease and other neurodegenerative diseases. *Nutrients* **10**, 708(2018).
32. Fan, H.-X., Sheng, S. & Zhang, F. New hope for Parkinson's disease treatment: targeting gut microbiota. *CNS Neurosci. Ther.* **28**, 1675–1688 (2022).
33. Gagliardi, A. et al. Rebuilding the gut microbiota ecosystem. *Int. J. Environ. Res. Public Health* **15**, 1679 (2018).
34. Trinder, M., Daisley, B. A., Dube, J. S. & Reid, G. Drosophila melanogaster as a high-throughput model for host-microbiota interactions. *Front. Microbiol.* **8**, 1–8 (2017).
35. Partridge, L., Piper, M. D. W. & Mair, W. Dietary restriction in Drosophila. *Mech. Ageing Dev.* **126**, 938–950 (2005).
36. Koyle, M. L. et al. Rearing the fruit fly drosophila melanogaster under axenic and gnotobiotic conditions. *J. Vis. Exp.* **30**, 54219 (2016).
37. Chiang, M. H. et al. Drosophila model for studying gut microbiota in behaviors and neurodegenerative diseases. *Biomedicines* **10**, 596 (2022).
38. Torres-Miranda, A., Melis-Arcos, F. & Garrido, D. Characterization and identification of probiotic features in lacticaseibacillus paracasei using a comparative genomic analysis approach. *Probiotics Antimicrob. Proteins* **14**, 1211–1224 (2022).
39. Paricio, N. & Muñoz-Soriano, V. Drosophila models of Parkinson's disease: discovering relevant pathways and novel therapeutic strategies. *Parkinsons Dis.* **2011**, 520640 (2011).
40. Feany, M. B. & Bender, W. W. A Drosophila model of Parkinson's disease. *Nature* **404**, 394–398 (2000).
41. Mohite, G. M. et al. Parkinson's Disease associated α-synuclein familial mutants promote dopaminergic neuronal death in drosophila melanogaster. *ACS Chem. Neurosci.* **9**, 2628–2638 (2018).
42. Cao, W. et al. An automated rapid iterative negative geotaxis assay for analyzing adult climbing behavior in a Drosophila model of neurodegeneration. *J. Vis. Exp.* **2017**, 5–9 (2017).
43. Havelund, J. F., Heegaard, N. H. H., Færgeman, N. J. K. & Gramsbergen, J. B. Biomarker research in parkinson's disease using metabolite profiling. *Metabolites* **7**, 42, (2017).
44. Figura, M. et al. Serum amino acid profile in patients with Parkinson's disease. *PLoS ONE* **13**, e0191670 (2018).
45. Li, X., Fan, X., Yang, H. & Liu, Y. Review of metabolomics-based biomarker research for parkinson's disease. *Mol. Neurobiol.* **59**, 1041–1057(2022).

46. Le Bourg, E. & Lints, F. A. Hypergravity and aging in Drosophila melanogaster. 4. Climbing activity. *Gerontology* **38**, 59–64 (1992).

47. Buck, S. A. et al. Vesicular glutamate transporter modulates sex differences in dopamine neuron vulnerability to age-related neurodegeneration. *Aging Cell* **20**, e13365 (2021).

48. Chaudhuri, A. et al. Interaction of genetic and environmental factors in a Drosophila Parkinsonism model. *J. Neurosci.* **27**, 2457 (2007).

49. Bayersdorfer, F., Voigt, A., Schneuwly, S. & Botella, J. A. Dopamine-dependent neurodegeneration in Drosophila models of familial and sporadic Parkinson's disease. *Neurobiol. Dis.* **40**, 113–119 (2010).

50. Bloem, B. R., Okun, M. S. & Klein, C. Parkinson's disease. *Lancet* **397**, 2284–2303(2021).

51. Singh, Y. P., Pandey, A., Vishwakarma, S. & Modi, G. A review on iron chelators as potential therapeutic agents for the treatment of Alzheimer's and Parkinson's diseases. *Mol. Divers* **23**, 509–526 (2019).

52. Anandhan, A. et al. Metabolic dysfunction in Parkinson's disease: bioenergetics, redox homeostasis and central carbon metabolism. *Brain Res. Bull.* **133**, 12–30 (2017).

53. Kalecký, K. & Bottiglieri, T. Targeted metabolomic analysis in Parkinson's disease brain frontal cortex and putamen with relation to cognitive impairment. *NPJ Parkinsons Dis.* **9**, 84 (2023).

54. Solana-Manrique, C. et al. Metabolic alterations in a drosophila model of parkinson's disease based on DJ-1 deficiency. *Cells* **11**, 1–17 (2022).

55. Murali Mahadevan, H., Hashemiaghdam, A., Ashrafi, G. & Harbauer, A. B. Mitochondria in neuronal health: from energy metabolism to Parkinson's disease. *Adv. Biol.* **5**, e2100663 (2021).

56. Tosukhowong, P. et al. Biochemical and clinical effects of Whey protein supplementation in Parkinson's disease: a pilot study. *J. Neurol. Sci.* **367**, 162–170 (2016).

57. Reiterer, M., Schmidt-Kastner, R. & Milton, S. L. Methionine sulfoxide reductase (Msr) dysfunction in human brain disease. *Free Radic Res.* **53**, 1144–1154 (2019).

58. Oien, D. B., Shinogle, H. E., Moore, D. S. & Moskovitz, J. Clearance and phosphorylation of alpha-synuclein are inhibited in methionine sulfoxide reductase a null yeast cells. *J. Mol. Neurosci.* **39**, 323–332 (2009).

59. Liu, F. et al. Methionine sulfoxide reductase A protects dopaminergic cells from Parkinson's disease-related insults. *Free Radic. Biol. Med.* **45**, 242–255 (2008).

60. Catanesi, M. et al. L-methionine protects against oxidative stress and mitochondrial dysfunction in an in vitro model of parkinson's disease. *Antioxidants* **10**, 1467 (2021).

61. Boertien, J. M., Pereira, P. A. B., Aho, V. T. E. & Scheperjans, F. Increasing comparability and utility of gut microbiome studies in parkinson's disease: a systematic review. *J. Parkinsons Dis.* **9**, S297–S312 (2019).

62. Sampson, T. R. et al. Gut microbiota regulate motor deficits and neuroinflammation in a model of Parkinson's disease. *Cell* **167**, 1469–1480.e12 (2016).

63. Parker-Character, J. et al. An altered microbiome in a Parkinson's disease model Drosophila melanogaster has a negative effect on development. *Sci. Rep.* **11**, 23635(2021).

64. Li, C. et al. Gut microbiota differs between parkinson's disease patients and healthy controls in northeast China. *Front Mol. Neurosci.* **12**, 171 (2019).

65. Bashir, Y. & Khan, A. U. The interplay between the gut-brain axis and the microbiome: a perspective on psychiatric and neurodegenerative disorders. *Front Neurosci.* **16**, 1030694 (2022).

66. Pascale, A., Marchesi, N., Govoni, S. & Barbieri, A. Targeting the microbiota in pharmacology of psychiatric disorders. *Pharmacol Res.* **157**, 104856 (2020).

67. Chen, Y., Xu, J. & Chen, Y. Regulation of neurotransmitters by the gut microbiota and effects on cognition in neurological disorders. *Nutrients* **13**, 2099 (2021).

68. Sears, S. M. S. & Hewett, S. J. Influence of glutamate and GABA transport on brain excitatory/inhibitory balance. *Exp. Biol. Med.* **246**, 1069–1083 (2021).

69. Zhang, F. Q., McMullen, J. G., Douglas, A. E. & Ankrah, N. Y. D. Succinate: A microbial product that modulates *Drosophila* nutritional physiology. *Insect. Sci.* **29**, 315–318(2022).

70. Tan, F. H. P. et al. Lactobacillus probiotics improved the gut microbiota profile of a Drosophila melanogaster Alzheimer's disease model and alleviated neurodegeneration in the eye. *Benef. Microbes* **11**, 79–90 (2020).

71. Liu, G. et al. Lactic acid bacteria feeding reversed the malformed eye structures and ameliorated gut microbiota profiles of Drosophila melanogaster Alzheimer's disease model. *J. Appl. Microbiol.* **132**, 3155–3167 (2022).

72. Wang, L. et al. Lactobacillus plantarum DP189 reduces α-SYN aggravation in MPTP-induced Parkinson's disease mice via regulating oxidative damage, inflammation, and gut microbiota disorder. *J. Agric. Food Chem.* **70**, 1163–1173 (2022).

73. Medina, D. A., Pinto, F., Ovalle, A., Thomson, P. & Garrido, D. Prebiotics mediate microbial interactions in a consortium of the infant gut microbiome. *Int. J. Mol. Sci.* **18**, 2095 (2017).

74. Bolger, A. M., Lohse, M. & Usadel, B. Trimmomatic: a flexible trimmer for Illumina sequence data. *Bioinformatics* **30**, 2114–2120 (2014).

75. Prjibelski, A., Antipov, D., Meleshko, D., Lapidus, A. & Korobeynikov, A. Using SPAdes de novo assembler. *Curr. Protoc. Bioinform.* **70**, e102 (2020).

76. Arkin, A. et al. KBase: The United States department of energy systems biology knowledgebase. *Nat. Biotechnol.* **36**, 566–569, https://doi.org/10.1038/nbt.4163 (2018).

77. Heirendt, L. et al. Creation and analysis of biochemical constraint-based models using the COBRA Toolbox v.3.0. *Nat. Protoc.* **14**, 639–702 (2019).

78. Magnúsdóttir, S. et al. Generation of genome-scale metabolic reconstructions for 773 members of the human gut microbiota. *Nat. Biotechnol. VOLUME* **35**, 81–89 (2017).

79. Hirmas, B. et al. Metabolic modeling and bidirectional culturing of two gut microbes reveal cross-feeding interactions and protective effects on intestinal cells. *MSystems* **7**, e0064622 (2022).

80. Chan, S. H. J., Simons, M. N. & Maranas, C. D. SteadyCom: Predicting microbial abundances while ensuring community stability. *PLoS Comput Biol* **13**, e1005539 (2017).

81. Duncan, S. H., Barcenilla, A., Stewart, C. S., Pryde, S. E. & Flint, H. J. Acetate utilization and butyryl coenzyme A (CoA): Acetate-CoA transferase in butyrate-producing bacteria from the human large intestine. *Appl. Environ. Microbiol.* **68**, 5186–5190 (2002).

82. Gutiérrez, N. & Garrido, D. Species deletions from microbiome consortia reveal key metabolic interactions between gut microbes. *MSystems* **4**, 1–16 (2019).

83. Watchararparpaiboon, W., Laohakunjit, N. & Kerdchoechuen, O. An improved process for high quality and nutrition of brown rice production. *Food Sci. Technol. Int.* **16**, 147–158 (2010).

84. Agostini, F., Bubacco, L., Chakrabarti, S. & Bisaglia, M. α-synuclein toxicity in drosophila melanogaster is enhanced by the presence of iron: implications for parkinson's disease. *Antioxidants* **12**, 261 (2023).

85. Xue, J., Wang, H. L. & Xiao, G. Transferrin1 modulates rotenone-induced Parkinson's disease through affecting iron homeostasis in Drosophila melanogaster. *Biochem. Biophys. Res. Commun.* **531**, 305–311 (2020).

86. Doktór, B., Damulewicz, M. & Pyza, E. Overexpression of mitochondrial ligases reverses rotenone-induced effects in a Drosophila model of Parkinson's disease. *Front Neurosci.* **13**, 1–10 (2019).

87. Schneider, C. A., Rasband, W. S. & Eliceiri, K. W. NIH image to imageJ: 25 years of image analysis. *HHS Public Access* **9**, 671–675 (2012).

88. López del Amo, V. et al. A Drosophila model of GDAP1 function reveals the involvement of insulin signalling in the mitochondria-dependent neuromuscular degeneration. *Biochim. Biophys. Acta Mol. Basis Dis.* **1863**, 801–809 (2017).

89. Pang, Z. et al. MetaboAnalystR 4.0: a unified LC-MS workflow for global metabolomics. *Nat. Commun.* **15**, 3675 (2024).

90. Bolyen, E. et al. Reproducible, interactive, scalable and extensible microbiome data science using QIIME 2. *Nat. Biotechnol.* **37**, 852–857 (2019).

91. Team R. A *Language And Environment For Statistical Computing. Computing;1*. https://www.r-project.org/ (2006).

92. Callahan, B. J. et al. DADA2: High-resolution sample inference from Illumina amplicon data. *Nat Methods* **13**, 581–583(2016).

93. DeSantis, T. et al. Greengenes, a chimera-checked 16S rRNA gene database and workbench compatible with ARB. *Appl. Environ. Microbiol. AEM* **72**, 5069–5072 (2006).

94. Anders, S. & Huber, W. Differential expression analysis for sequence count data. *Genome Biol* **11**, R106(2010).

Acknowledgements

Author contributions

A.O.: Conceptualization, Methodology, Investigation, Software, writing original draft, writing review, and editing. E.L.: Investigation, Methodology. D.G.: Conceptualization, Investigation, writing original draft, writing review and editing, Resources, and Supervision. JS: Conceptualization, Investigation, writing review and editing, Resources, and Supervision. N.P.: Writing—review and editing, Resources, and Supervision.

Competing interests

The authors declare no competing interests.

Additional information

Supplementary information The online version contains supplementary material available at https://doi.org/10.1038/s41522-025-00797-5.

Correspondence and requests for materials should be addressed to Jimena Sierralta, Nuria Paricio or Daniel Garrido.

Reprints and permissions information is available at http://www.nature.com/reprints

Publisher's note Springer Nature remains neutral with regard to jurisdictional claims in published maps and institutional affiliations.